

Characterization, microstructure and properties of fly ash-based geopolymer

S. Alehyen, M. EL Achouri, M. Taibi

*Laboratoire de Physico-Chimie des Matériaux Inorganiques et Organiques
Ecole Normale Supérieure- Rabat, Mohammed V University -Rabat-Morocco*

Received 20 Jan 2017,
Revised 13 Feb 2017,
Accepted 15 Feb 2017

Keywords

- ✓ Fly ash
- ✓ geopolymer
- ✓ alkaline activation
- ✓ characterization microstructure
- ✓ Thermal stability
- ✓ Chemical stability
- ✓ Water absorption

alehyensali@yahoo.fr

Abstract

This work is dealing with the valorization of Moroccan fly ash produced by the coal-fired Jorf Lasfar plant in the preparation of fly ash based geopolymer by alkaline activation. Sodium hydroxide and sodium silicate in appropriate ratio were used as an alkaline activator. The characterization of the raw material and the fly ash - based geopolymer synthesized was undertaken using several analytical methods such as XRD, FTIR, FX and ^{29}Si MAS-RMN. Microstructure studies have been conducted using SEM Microscopy. The result of XRD analysis shows that the geopolymer exhibits an amorphous character with minority crystalline phase. The FTIR Spectra analysis reveals that the spectral band corresponding to Si-O and Al-O is displaced towards lower values. This shift is interpreted as a consequence of the Al penetration into the original structure of the Si-O-Si skeleton as observed analogously in zeolites. According to ^{29}Si RMN MAS investigation, the fly ash based geopolymer contains mainly structures of the types Q_4 (2Al) and Q_4 (3Al). The microstructure of geopolymer specimens reveals the formation of heterogeneous matrix which consists of a dense continuous gel-like with microcracks and micropores. Thermal stability of fly ash based geopolymer was studied using DSC Calorimetry and shows that the geopolymer possess high thermal properties. The chemical stability was studied by zetametry, the large negative value of zeta potential obtained indicates the high stability of geopolymer suspensions. Water absorption properties were also undertaken and show that the water absorption of geopolymer paste is lower than that of ordinary portland Cement control samples.

1. Introduction

Geopolymer is a class of inorganic polymers formed by reacting silica-rich and alumina-rich solids with a high alkaline solution, which combines the properties of polymers, ceramics and cements [1-2]. Nowadays, geopolymer studies are receiving note worthily increasing attention because they may be used as a viable economical alternative to organic polymers and inorganic cements in diverse applications, such as aircraft [3-4], high-tech ceramics [5], thermal insulating foams [5], fire-proof building materials [6], protective coatings [1], refractory adhesives [7] and hybrid inorganic-organic composites [8-9]. This interest is due to their exceptionally high thermal and chemical stability, excellent mechanical strength, adhesive behavior and long-term durability.

Geopolymer are amorphous to semi-crystalline equivalent of certain zeolitic materials with excellent properties, such as high fire and erosion resistances, and high strength materials. Recent works have shown that the addition of moderate amount of minerals to a geopolymer can give significant improvements on the geopolymer structure and properties [10]. The alkaline activation of materials can be defined as a chemical process that provides a rapid change of some specific structures, partial or totally amorphous, into compact cemented frameworks [11]. Some researchers described the alkali activation of fly ash as a physical-chemical process in which this powdery solid is mixed with a concentrated alkali solution in a suitable proportion to produce a workable and mouldable paste and stored at mild temperatures ($< 100^\circ\text{C}$) for a short period of time to produce a material with good binding properties [12-13]. At the end of this process, an amorphous alkaline aluminosilicate gel is formed as the main reaction product. In addition, Na- Herschel-type zeolites and hydroxysodalite are formed as secondary reaction products [14].

Many industrial by-products and other kinds of minerals can be used to produce the geopolymers [15-16]. The geopolymerization reaction is very sensitive to different raw materials (particle size and distribution, crystallization degree), nature of alkali-activators (Sodium/potassium hydroxide, Sodium/potassium silicate, the

ratio of these two), Si/Al ratios, water/ash ratios, curing conditions (temperature, moisture degree, opening or healing condition, curing time).

The chemical composition of geopolymer material is similar to natural zeolitic materials, but the microstructure is amorphous instead of crystalline [17-18]. According to Davidovits [1], geopolymers possess amorphous to semi-crystalline three dimensional silico-aluminate structures consisting of linked SiO₄ and AlO₄ tetrahedra by sharing the oxygen atoms, which can be designated as poly-sialate (-Si-O-Al-O-) (Si:Al = 1), poly-sialate-siloxo (-Si-O-Al-O-Si-O-) (Si:Al = 2), poly-sialate-disiloxo (-Si-O-Al-O-Si-O-Si-O-) (Si:Al = 3), and sialate links (Si:Al > 3). The sialate is an abbreviation for silicon-oxo-aluminate.

Fly ash is a by-product from the coal industry, which is widely available in the world. Fly ash is rich in silicate and alumina, hence it reacts with alkaline solution to produce aluminosilicate gel that binds the aggregate to produce a good geopolymer concrete. The compressive strength increases with the increasing of fly ash fineness and thus the reduction in porosity can be obtained. Fly ash based geopolymer also provided better resistance against aggressive environment and elevated temperature compared to normal concrete. The properties of fly ash-based geopolymer are enhanced with few factors that influence its performance [19-20]. Al Bakri et al [21] studied the effect of various molarity of NaOH to fly ash geopolymer paste. The properties of the geopolymer such as compressive strength, water absorption, porosity, and density were determined. The authors concluded that fly ash-based geopolymer with 12 M NaOH concentration shows excellent results with high compressive strength. Palomo et al [22] reported the study of fly ash-based geopolymers. They used combinations of sodium hydroxide with sodium silicate and potassium hydroxide with potassium silicate as alkaline liquids. It was found that the type of alkaline liquid is a significant factor affecting the mechanical strength and that the combination of sodium silicate and sodium hydroxide gave the highest compressive strength. The use of fly ash as a starting material provides cost and environmental benefits in comparison with other thermally prepared natural raw materials (e.g., metakaolin), since it has a lower incorporated energy and low CO₂ emission [23]. Fly ash appears to be the most promising precursor for large-scale industrial production of geopolymer products due to its high workability and low water demand [24].

Treatment and removal of fly ash as a waste from coal based power plants is an uneconomical and environment unfriendly task. Reutilization is mostly focused as pozzolanic material and about 10-15% of fly ash is used by cement industry. Dumping in lowlands is the most common practice used for discarding of fly ash causing water, land and aerial contamination. In the recent years, there has been a higher awareness on the hazardous solid waste generation and its impact on human health, as well as an increased focus on the environmental consequences of waste disposal. This forces the industry to find alternative ways to reuse waste materials. One solution is to reuse the waste materials to create geopolymers as an alternative to Portland cement.

The objective of this work is the valorization of fly ash generated by Moroccan power plant in the synthesis of fly ash based geopolymer. The fly ash used was supplied by Jorf lasfar power plant in Morocco. The composition, structure, microstructure and texture of the fly ash based geopolymer were investigated using several methods. The current work uses XRD, FTIR and ²⁹Si MAS NMR techniques to characterize fly ash in order to gain a greater understanding on phase composition and structure of fly ash-based geopolymeric materials. Some properties of geopolymers derived from fly ash have also been studied, namely thermal stability, chemical stability and water absorption. The thermal and chemical stability were investigated respectively by differential scanning calorimetry and zetametry. The water absorption experiments were performed by water immersion.

2. Experimental

2.1. Materials

The materials used for the synthesis of fly ash-based geopolymer paste specimens are fly ash as the source material, alkaline liquid activator and water.

2.1.1. Fly ash

Fly ash used in this study was low-calcium (ASTM Class F) dry fly ash from Jorf Lasfar power plant in Morocco.

2.1.2. Alkaline liquid activator

The alkaline liquid used was a combination of sodium silicate powder and sodium hydroxide solution. Na₂SiO₃ powder (18% Na₂O and 63% SiO₂) is purchased from Riedel –de-Haen and NaOH pellets (purity > 97%) is purchased from Fluka.

The NaOH solids pellets were dissolved in water to make the alkaline solution. The concentration of the NaOH solution used was 12M. This concentration was based on previous research [21] that indicated that the maximum strength of geopolymer was obtained when 12 M NaOH was used. The alkaline liquid was prepared by mixing a sodium silicate Na_2SiO_3 and NaOH in the mass ratio of 2.5. The sodium silicate powder and the sodium hydroxide solution were mixed together at least one day prior to use as alkaline liquid.

2.1.3. Mixture Proportion

The geopolymer paste was prepared by mixing fly ash with alkaline mixture in a solid to liquid ratio of 2.5. Extra water is added to have the desired workability of the geopolymer paste. The mixture proportions of geopolymer paste were given in Table 1.

Table1 . Mixture proportions of geopolymer paste

Mixture of geopolymer	Mass (g), Ratio
Mass of fly ash(g)	100
Mass of NaOH (g)	11.43
Mass of Na_2SiO_3 (g)	28.57
Mass of water of NaOH dilution (g)	23.81
Extra water(g)	10
Total water(g)	33.81
%fly Ash	71.4
Ratio water/fly ash	0.34
Ratio fly ash/alkaline activator	2.5
Ratio $\text{Na}_2\text{SiO}_3/\text{NaOH}$	2.5

2.1.4. Curing process

After mixing, the geopolymer paste was cast in a cylindrical plastic mould and left for 24h at the temperature of 70°C. After the curing period, the test specimens were left in the moulds for at least six hours. After demoulding, the specimens were left to air-dry in the laboratory until the day of test.

2.2. Methods

2.2.1. Fluorescence X-Ray Spectroscopy (XRF)

Fluorescence X-Ray analysis was performed using wavelength dispersive (WDXRF) spectrometer Axios type.

2.2.2. X-Ray Diffraction (XRD)

The different diffraction patterns of fly ash and geopolymer were obtained on a device Xpert -Pro diffractometer using $\text{Cu K}\alpha_1$ radiation ($\lambda = 1.54056 \text{ \AA}$). The analytical range is between 3 and 90 ° with a step of 0.06 °. The crystalline phases present in the material are identified by comparison with the standard PDF (Powder Diffraction Files) of CSDI (International Center for Diffraction Data).

2.2.3. Fourier Transform Infrared spectroscopy analysis (FTIR)

The consolidated geopolymers materials are mainly composed of the elements silicon, aluminum and alkali cation. The presence of these three elements will induce a large number of possible linkages (Si-O-Si, Si-O-Al, Si-O, Si-O-M, O-Si-O where M = Na), each having different vibrational modes. The measurements by infrared spectroscopy were carried out on an apparatus VERTEX 70 in MIR transmission mode in the wave number region from 400 to 4000 cm^{-1} .

2.2.4. Magic -Angle Spinning Nuclear Magnetic Resonance Spectroscopy (^{29}Si MAS -NMR)

The study of fly ash and consolidated materials was carried out by MAS NMR Silicon (Magic Angle Spinning) . ^{29}Si MAS-NMR spectroscopic characterization was conducted with a Bruker apparatus, model Avance III 600 MHz. The spectrometer used has a main field magnetic 14 Tesla. The measurements were taken at laboratory temperature with TMS as the external standard. The error in the chemical shift values was estimated to be lower than 1 ppm. Magnetic materials were removed from the samples prior to NMR spectra recording by exposing the sample to a strong magnetic field.

2.2.5. Scanning Electron Microscopy analysis (SEM)

Scanning Electron Microscopy (SEM) is a surface characterization technique allowing observations to the nanoscale. Before being observed by SEM, a deposit gold / palladium (Au / Pd) is performed on the samples. This metallization prevents the accumulation of charge at the surface of the sample and reduces the penetration depth of the beam, thereby improving the image quality. Microstructural investigations of the geopolymer paste were carried out using the FEI quanta 450 FEG focused- ion-beam system, equipped with an EDAX Genesis energy dispersive spectrometer (EDS) at Moroccan Foundation for Advanced Science, Innovation and Research (Mascir).

2.2.6. Differential Scanning Calorimetry analysis (DSC)

Differential Scanning Calorimetry (DSC) is a thermal technique used to measure the difference of heat exchange between a sample and a reference. The resulting curve showing the heat emitted or absorbed by the material versus the temperature provides information on the phase transitions: glass transition temperature, the melting and crystallization temperatures and enthalpies of reaction. The experimental conditions were:

- Device Type: DSC SETARAM121
- Sample mass : 10 to 30 mg
- Temperature rise : 30°C to 800°C
- Test atmosphere : argon
- Heat rate:10°C/min

2.2.7. Zetametry study

Malvern Zetasizer (nano series) was used to measure the zeta potential of geopolymer matrices well-dispersed in deionized water (5% weight suspension). Before each set of measurements, the instrument was calibrated using potassium tungstosilicate solution, and all calculations were performed using the Zetasizer software. The method used is the Dynamic Light Scattering (DLS).

2.2.8. Water Absorption

By definition (ASTM D 2216 – 05 2005), water content, w , is the ratio of the mass of water contained in the pore spaces of material to the solid mass of particles in the material, which is expressed as a percentage. The standard and recommended method for determining the water content of material is the oven-drying method with a drying temperature of 110 ± 5 °C. The water content of a material is used in expressing the phase relationships of air, water and solids in a given volume of material. The water content, w , is calculated as follows (ASTM D 2216 - 05):

$$W = \frac{M_{cms} - M_{c ds}}{M_{c ds} - M_c} * 100 = \frac{M_w}{M_s} * 100$$

M_{cms} = mass of container and moist specimen, g, $M_{c ds}$ = mass of container and oven dry specimen, g, M_c = mass of container, g, M_w = mass of water, g, and M_s = mass of oven dry specimen,g.

3. Results and Discussion

3.1. Characterisation and Microstructure

3.1.1. FX analysis

3.1.1.1. Fly ash

Fly ash is a finely divided residue resulting from the combustion of ground or powdered coal in electricity generating plant. Fly ash consists of minerals, which include silicon, aluminum, iron, calcium, magnesium and traces of titanium and organic matter, such as carbon. It is being regarded as coal combustion waste. The chemical composition of Jorf Lasfar fly ashes used in this study obtained by X-Ray Fluorescence spectroscopy (XRF) is given in Table 2.

Table 2. Chemical composition of fly ash

Constituent	LOI	SiO ₂	Al ₂ O ₃	Fe ₂ O ₃	CaO	K ₂ O	Na ₂ O	TiO ₂	SO ₃	P ₂ O ₅
%	7.12	52.5	30.2	2.94	0.822	2.08	0.719	1.03	0.787	0.203
Costituent	MgO	Rb	SrO	BaO	ZrO ₂	Nb ₂ O ₅	CuO	ZnO		
%	1.23	0.0694	0.0518	0.0484	0.0382	0.0156	0.0137	0.0126		

LOI : loss of ignition

According to Table 2, Jorf lasfar fly ashes includes substantial amounts of silicon dioxide (SiO₂) and aluminum

oxide (Al_2O_3). Calcium oxide (CaO), iron oxide (Fe_2O_3), magnesium, potassium, sodium, titanium and sulphur are also present in lesser amount. The silicon and aluminum constitute about 80% of the total mass ($\text{SiO}_2 + \text{Al}_2\text{O}_3 = 82.7\%$) and the percentage of calcium oxide was less than 10%. Therefore, the Jorf Lasfar fly ash was referred as ASTM Class F fly ash or low calcium fly ash. The ratio of silicon to aluminum oxide is about 1,

3.1.1.2. Fly ash based Geopolymer

The chemical composition of geopolymer is given in the Table 3. The major constituents of fly ash based geopolymer were the silicon, the sodium and aluminum oxides. Indeed, these components represented 82% of the total mass of geopolymer. The greater difference between the composition of fly ash and geopolymer is in the high content of sodium oxide in the geopolymer which originates from the alkaline activator.

Table 3. Chemical composition of Fly ash- geopolymer

Constituent	LOI	SiO_2	Na_2O	Al_2O_3	Fe_2O_3	K_2O	TiO_2	MgO	CaO	SO_3
%	5.82	37.8	28.3	15.9	4.67	2.65	1.58	1.18	1.15	0.37
Constituent	P_2O_5	SrO	BaO	ZrO_2	CuO	Nb_2O_5	CuO	ZnO	Rb	
%	0.1	0.0896	0.0882	0.0666	0.0345	0.0341	0.0137	0.0338	0.027	

3.1.2. X-ray Diffraction (XRD)

3.1.2.1. XRD pattern of Fly ash

The basic material of Jorf Lasfar fly ash is of a prevailing amorphous character only seldom containing needle-shaped minority crystals. The X-ray diffraction (XRD) pattern of fly ash shown in Figure 1a, which illustrates the crystalline phases present in the fly ash namely, quartz and mullite.

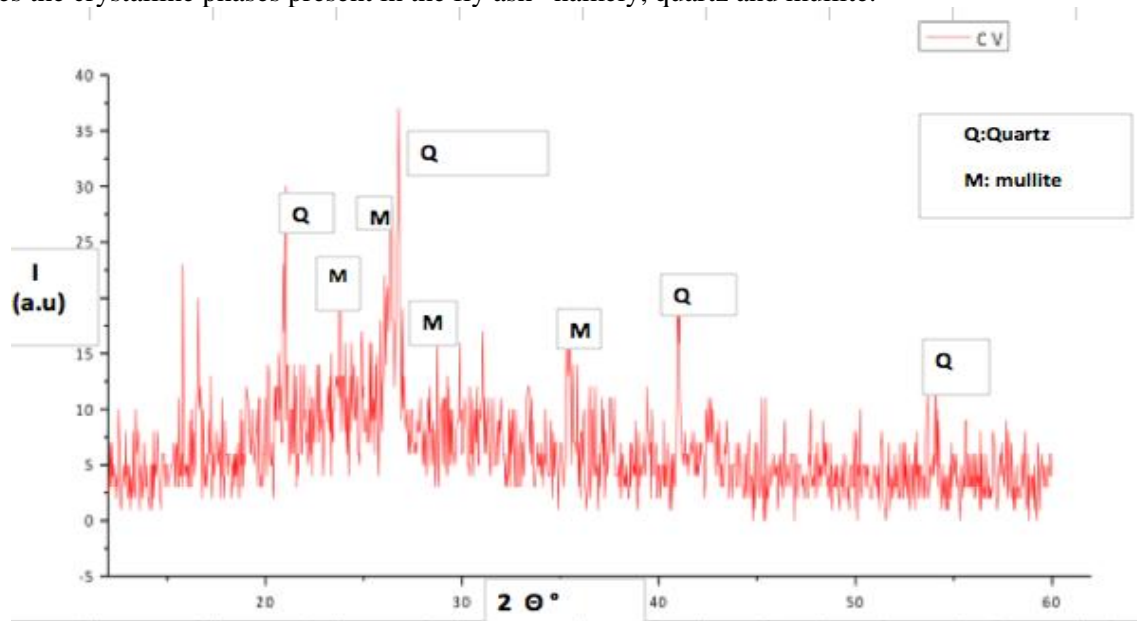


Figure 1 a: XRD pattern of Jorf Lasfar fly ash

Mullite (Alumina silicate) shows peaks at 25.82° , 27.20° of 2θ values (d spacing of 3.45 and 3.4 Å). The quartz exhibits peaks at 20.73° , 26.52° , 26.66° , 40.66° , 49.96° of 2θ values (d spacing of 4.28, 3.36, 3.34, 2.21, 1.82 Å). The presence of amorphous phases is identified as a broad diffraction 'hump' in the region between 14 to 30 degrees (2θ). The amorphous vitreous phase consists of amorphous silica and alumina.

3.1.2.2. XRD pattern of fly ash based Geopolymer

XRD patterns of fly ash based geopolymer illustrated in figure 1b shows that the geopolymer materials are prevailing of X-ray amorphous character where the diffraction crystals were those of the original materials : mullite and quartz. An amorphous hump is observed in the diffraction pattern between 2θ values of approximately 20° to 40° , which could be due to the presence of amorphous glassy materials.

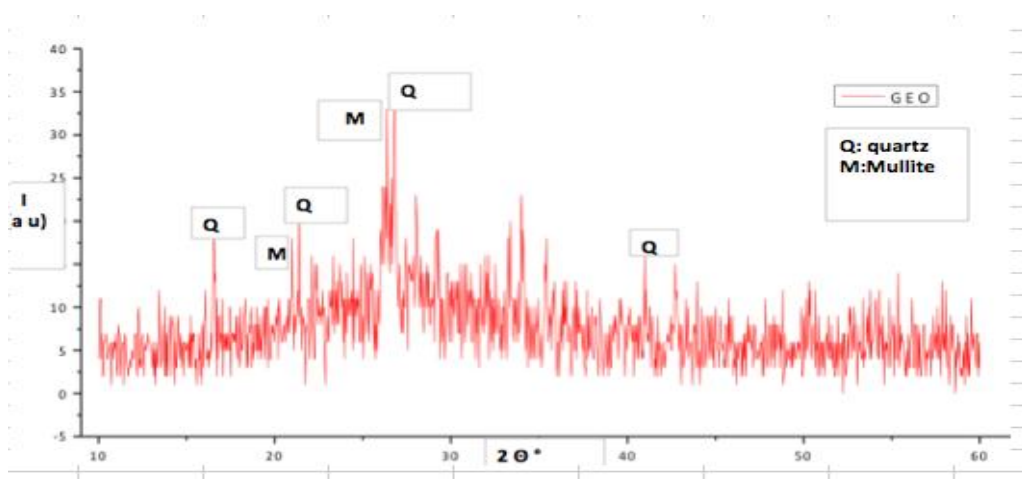


Figure 1b : XRD pattern of fly ash based geopolymer

The diffractogram for the original fly ash changed when the ash was activated by alkaline solutions. The hump, which is attributed to the vitreous phase of the original ash, slightly shifted from 14-30 ° to 20-40° (2θ) values. This change indicates the formation of an alkaline aluminosilicate hydrate gel N-A-S-H which has been identified as the primary reaction product of geopolymerization reaction in the diffraction patterns of geopolymeric materials [25-29]. The crystalline phases (quartz, mullite) detected in the initial material remained apparently unaltered with activation. For the geopolymer pattern, the original mineralogy of fly ash is not significantly modified. The N-A-S-H amorphous gel matrix results from the inter-geopolymerization of the fly ash glassy spheres with the alkaline solution.

3.1.3 FT-IR Analysis

Figures 2 a and b show the transmission mode of FT-IR spectra for fly ash and geopolymer samples, while Table 4 lists the position of wave numbers for molecular vibrations of different bonds that are present in fly ash and fly ash based geopolymer with their possible assignments.

3.1.3.1 Fly ash

The result of infrared spectroscopic for fly ash is shown in figure 2.a. The IR spectrum of fly ash shows transmission bands at 3441, 1622, 1383, 1075, 795, 558 and 459cm⁻¹. The main peaks are at 1075 and 459cm⁻¹.

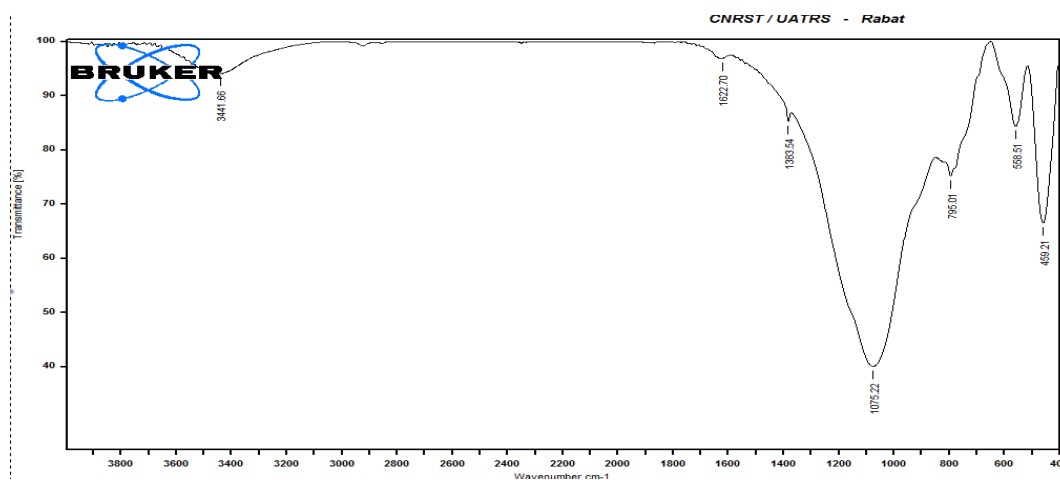


Figure 2
FTIR

a:

spectra of fly ash

3.1.3.2 Fly ash based geopolymer

The geopolymer spectra obtained is illustrated in Figure 2 b. The most important transmission bands are at 3432, 997 and 444 cm⁻¹. In geopolymer materials, a large broad band at 3400 cm⁻¹ is attributed to the presence of the O-H stretching frequency of silanol groups bonded to the inorganic structure, and also hydrogen bonds between adsorbed water and silanol group. The band at 1650 cm⁻¹ assigned to vibration of water

molecules bonded to the inorganic backbone. These bands indicate the presence silanol group Si-OH and bound water molecules in the geopolymer cement [30-32].

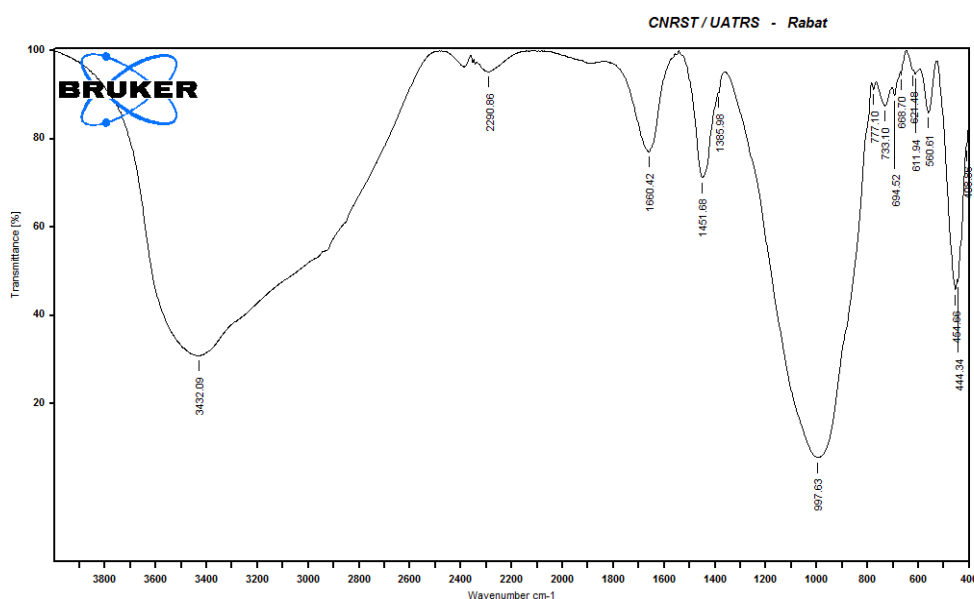


Figure 2 b : FT- IR spectra of fly ash based geopolymer

Table 4. Important IR bands of fly ash and geopolymer with their possible assignments

Wave number (cm ⁻¹)	Fly Ash	Geopolymer	Assignment
3441	+		OH groups of Si-OH and adsorbed water molecules on the surface of fly ash
3432		+	OH groups of Si-OH and adsorbed water molecules on the surface of fly ash geopolymer
2290			
1660		+	Stretching of H-O-H
1622	+		Stretching of O-H and H-O-H
1451		+	O-C-O stretching(Carbonates)
1075	+		Si-O-Si and Al-O-Si Asymmetric stretching
997		+	
894		+	Si-OH stretching
795	+		Al-O bending vibration
771		+	
733		+	
611		+	
558-560	+	+	Si-O-Si and Al-O-Si Asymmetric stretching
420-500	+	+	Si-O- and Al-O bending vibration

The main feature of the FTIR spectra of fly ash was the central band at around 1075 cm⁻¹, which is attributed to the Si-O-Si or Al-O-Si asymmetric stretching mode. The intensity of this band is proportional to the reactivity of fly ash [33]. This strong band shifts towards low wave number (997 cm⁻¹) in the geopolymeric cement, the shift is approximately 78 cm⁻¹. This demonstrates that an obvious change in the microstructure takes place during geopolymerization reaction resulting in a formation of new product with different microstructure. The large shift

towards the low wave number may be attributed to the partial replacement of SiO_4 specie by AlO_4 resulting in a change in the local chemical environment of Si-O bond [1]. A larger shift indicates higher degree of Al penetration from the glassy part of fly ash into the $(\text{SiO}_4)^{4-}$ skelton as observed analogously in zeolites [34-37]. Another band at around 1450 cm^{-1} appeared in the geopolymer sample, but is absent in the fly ash. This band is characteristic of the asymmetric CO_3 stretching mode, which suggests the presence of sodium carbonate as a result of the reaction between excess sodium and atmospheric carbon dioxide [31, 37].

3.1.4. ^{29}Si RMN MAS analysis

The majority of geopolymeric materials of practical interest are non-crystalline. Their structure cannot be investigated from XRD and FTIR alone. Nuclear Magnetic Resonance (MAS-NMR) spectroscopy provides better insight into the molecular framework.

Q_n (mAl) unit is the conventional notation to describe the structural units in aluminosilicates, where « n » represents the covalence number of the silicon center and « m » the number of Al surrounding one tetrahedral SiO_4 unit. In this way, if $n = 0, 1, 2, 3$ and 4 , then silicon is respectively in isolated mono-group (Q_0), in disilicates and chain end group (Q_1), in middle group in chains (Q_2), in sheets sites (Q_3) and in three-dimensional cross-linked site (Q_4). The letter « m » represents the number of aluminium atoms in the first covalence sphere of silicon, the number of Si-O-Al, sialate unit. In general, if there is no aluminium atom in the first covalence sphere of silicon, the notation becomes Q_0 .

Figure 5 gives the results of ^{29}Si MAS-NMR analysis of the Jorf Lasfar fly ash and fly ash geopolymer .

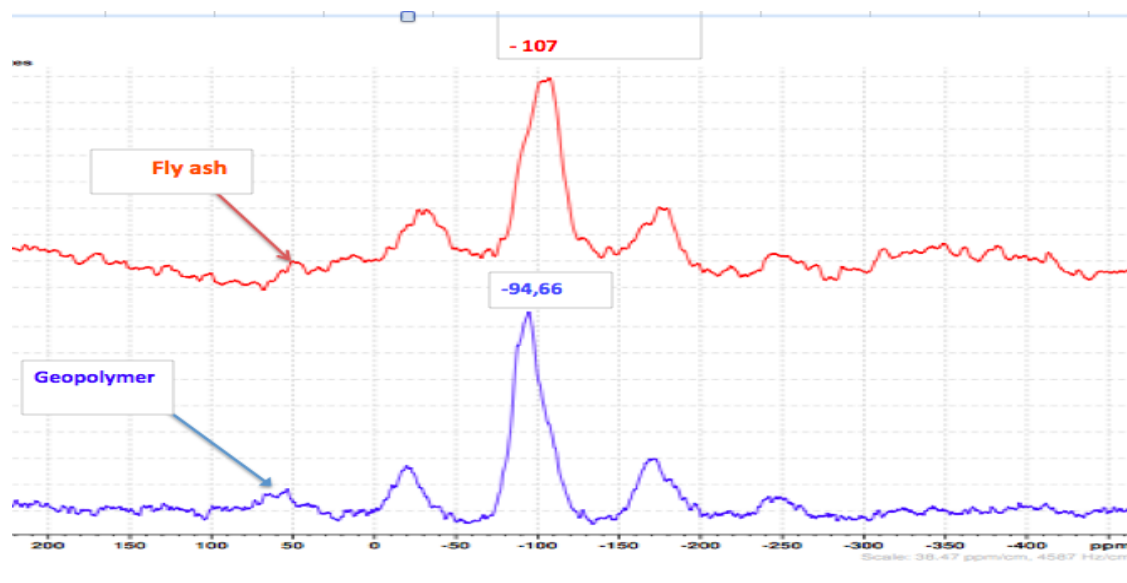


Figure 5 : ^{29}Si MAS –RMN spectra of fly and geopolymer.

The most prominent feature on these ^{29}Si NMR spectra for the fly ashes is a wide signal, indicative of the heterogeneous distribution of the Si atoms in this type of matrices. According to figure 5, The chemical shift equal to -107 ppm identified in ^{29}Si NMR MAS spectra of the fly ash is the most important and is attributed to the tetrahedral $[\text{SiO}_4]^{4-}$ coordination Q_4 [38-39].

According to the ^{29}Si RMN MAS spectra of fly ash based geopolymer , the main shift equal to $-94,66\text{ ppm}$ indicates the presence of $Q_4(2\text{ Al})$ and $Q_4(3\text{ Al})$ units in the geopolymer matrix [38]. The shift equal to -107 ppm corresponding to the $Q_4(0\text{ Al})$ coordination was less represented, which points to the Al penetration into the $[\text{SiO}_4]^{4-}$ skeleton. This interpretation of the NMR spectra is also shared by other workers [39-40]. Based on solid-state NMR-MAS study, the geopolymer contained exclusively tetraedrally coordinated silicon and aluminium. A basic conceptual view of geopolymer short-range ordering, incorporating only atomic connectivity proposed by Davidovits [29] is illustrated in Figure 6 a. Barbosa *et al* [25] proposed a new model for the molecular structure of geopolymer gel, whereby the framework structures are saturated in Al, e.g. $Q_4(3\text{ Al})$, as shown in Figure 6 ($Q_4(3\text{ Al})$ means there are 3 neighbouring Al atoms for a tetrahedral Si). The new model contains Si and Al tetrahedra which are randomly cross-linked to provide cavities, in order to accommodate the charge-balancing hydrated sodium ions.

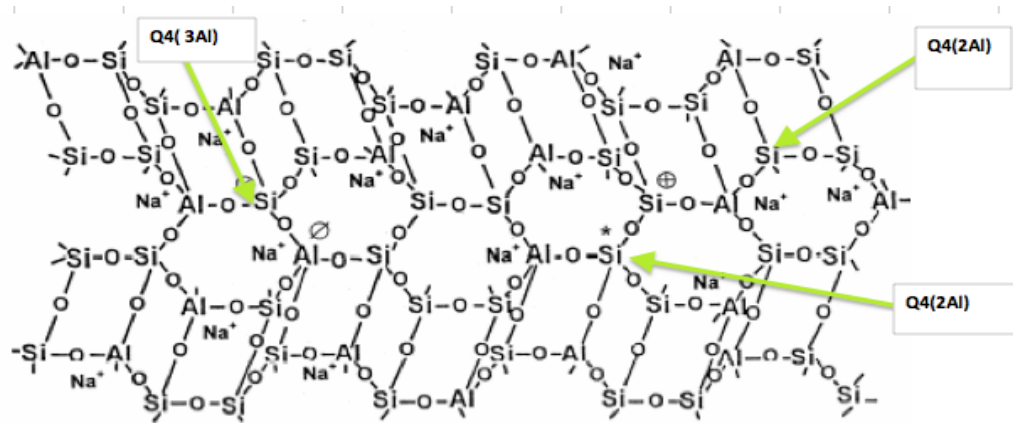


Figure 6 a : Conceptual model of geopolymer proposed by Davidovits [29]

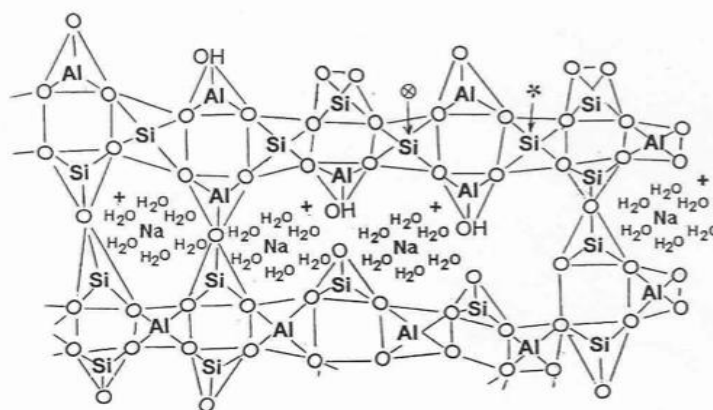


Figure 6 b : New model of geopolymer proposed by Barbosa et al [25]

3.1.5 Scanning Microscopy SEM analysis

3.1.5.1 Microstructure of Fly ash

The characteristic morphology of the original fly ash is shown in the SEM image in Figure 7, where it can be seen to consist of a series of spherical vitreous particles of different sizes. It shows also that fine solid spherical particles (microspheres) are contained by the large cenosphere particles (>50 μm) formed during the combustion process. The resulting macro particles are known as “plerosphere”. Crystalline phase is also observed in the microstructure of fly ash .

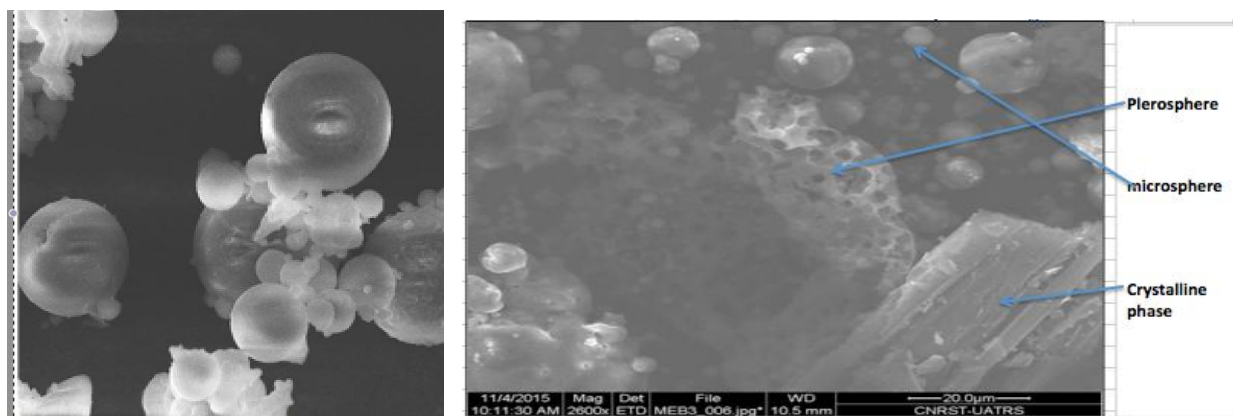


Figure 7 : SEM micrograph of fly ash

3.1.5.2 Microstructure of Fly ash based geopolymer

Figure 8 illustrates the SEM-determined microstructure characteristics of the prepared fly ash-based geopolymers synthesized at Fly Ash /alkaline activator ratio of 2,5.

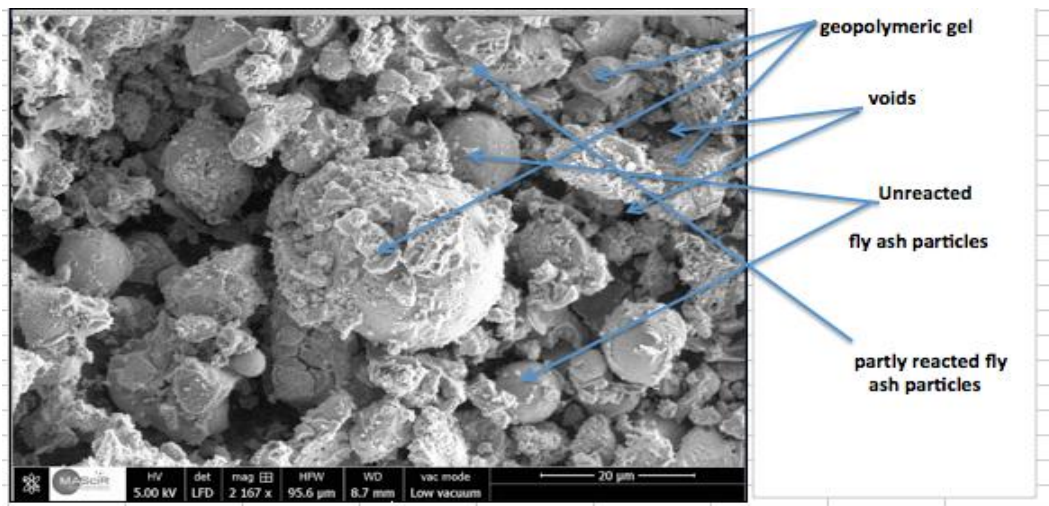


Figure 8: SEM micrograph of fly ash based geopolymer

According to micrograph illustrated in figure 8, the microstructure of Fly ash-based geopolymers is a porous, heterogeneous mixture of non- or partly-reacted fly ash grains, residual alkaline precipitates, and geopolymer gel. Figure 8 shows the microstructure of the fly ash based geopolymer in 12000 magnifications. The dense and bulky base is gel-like substances and can be characterized as geopolymer binders. It consists of a dense continuous gel-like with microcracks and micropores which can be clearly observed on the surface. The micro-crack shown in Figure 8 was caused by the drying shrinkage, a physical property, inherent of the gel. The gel shrinkage occurs because the removal of water during polycondensation creates capillary tension within the gel matrices [40].

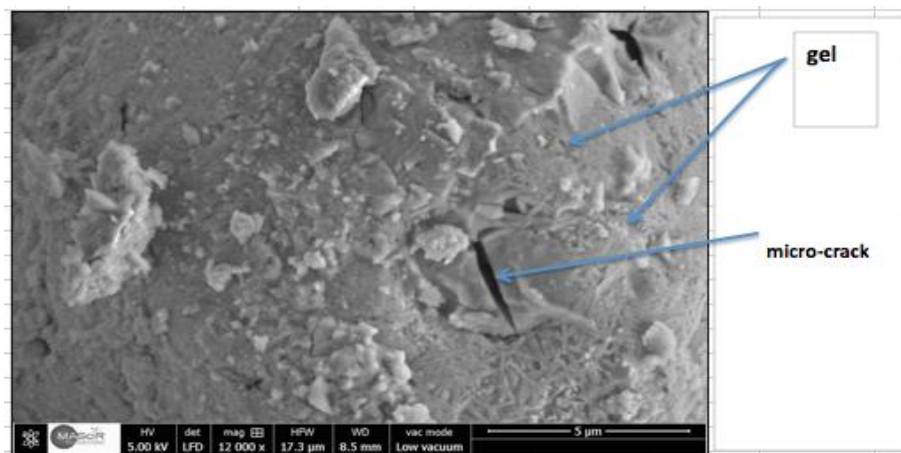


Figure 9: SEM micrographs of fly ash based geopolymer at 12000 magnification.

Figure 10 shows many needle or stripe-shaped particles which are formed in the surface of the geopolymer binder. The reason for the presence of many needle-shaped particles may be due to the high concentration or abundant alkali solution surrounded the fly ash ball in the geopolymer paste: the unreacted alkali precipitated after the tests and formed the needle or stripe-shaped particles. Figure 11 shows some small zeolites crystals formed in the surface of geopolymer as secondary products in geopolymerization process.

Based on the analysis of the microstructure of the fly ash geopolymer synthesized, the geopolymer products consist of many features: voids, pores, micro cracks, fly ash balls, dense and bulky geopolymer binders. The microspheres (originating from fly ash grains) are surrounded by a crust of reaction products. The adherence of the crust to the sphere does not appear to be very strong, and the bonding between grains is produced through the necks of the reaction products. The neo-formed needle or stripe-shaped particles indicate that the current geopolymer products may have the capability for the future growth of the compressive strength in the extended curing.

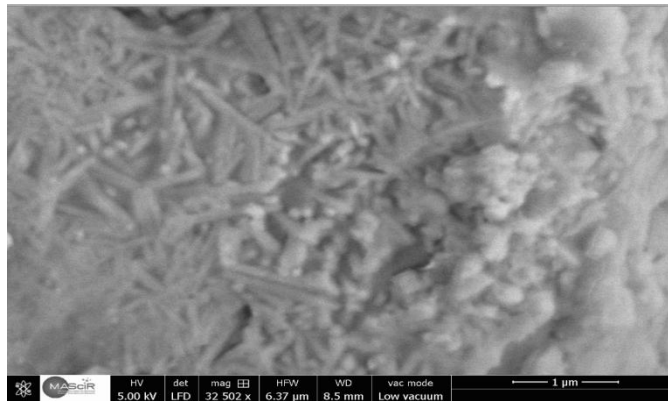


Figure 10 : SEM micrograph of fly ash geopolymer with many needles

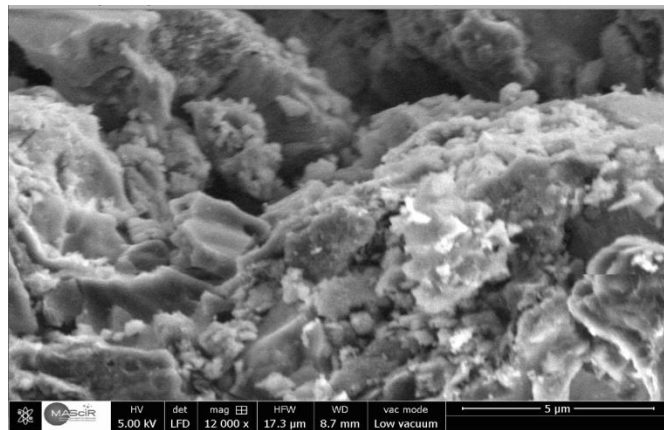


Figure 11: SEM micrograph of geopolymer with some small zeolites crystals

The reason for the presence of many needle-shaped particles may be due to the high concentration or abundant alkali solution surrounded the fly ash ball in the geopolymer paste. The porous microstructure leads to a good fire resistant performance. The geopolymer final products are continuous, bulky and dense geopolymer matrix with discrete pores and cracks. Two possible reasons are accounting for the cracks which are caused by the uneven internal stress or shrinkage due to the water evaporation during the curing. Small zeolites crystals are neoformed in the NASH gel which is the precursor of zeolites formation. The same results were obtained by others workers [22,41].

3.2. Properties of fly ash based geopolymer

3.2.1. Thermal Stability

The thermal stability was performed using Differential Scanning Calorimetry analysis. The DSC curves of fly ash and geopolymer were illustrated in figure 12.

DSC was used to measure a number of characteristic properties of fly ash and geopolymer pastes. Using this technique, it is possible to observe exothermic and endothermic events as well as glass transition temperatures. DSC curve of the geopolymer sample shows a remarkable endothermic peak centered at 85 °C. It is worth pointing out that the variation of enthalpy associated to removal of water. This fact indicates the presence of the weakly bound water molecules that were adsorbed on the surface or trapped in the large cavities between the rings of the geopolymeric products. According to the thermal study, the geopolymer exhibits a high thermal stability at elevated temperature in the range [0.800 ° C]. This result agrees with the finding Cheng and Chiu [42]. This fact confirms the excellent fire resistance of fly ash based geopolymer.

3.2.2. Chemical Stability by zetametry

Zeta potential is a scientific term for electrokinetic potential. It is a measure of the magnitude of the electrostatic or charge repulsion/attraction between particles, and is one of the fundamental parameters known to affect stability. The potential Zeta of the fly ash geopolymer was illustrated in Figure 13. The potential zeta of the fly ash geopolymer is equal to -41,6 mV. The large negative value of the zeta potential obtained reflects the high stability of the geopolymer suspensions.

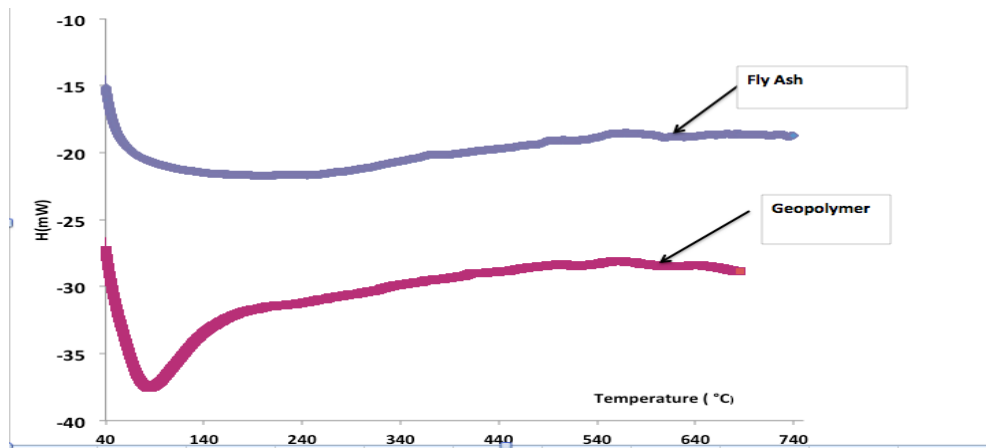


Figure 12 : DSC curves of fly ash and fly ash based geopolymer .

Results

	Mean (mV)	Area (%)	Width (mV)
Zeta Potential (mV): -41.6	Peak 1: -41.6	100.0	8.56
Zeta Deviation (mV): 8.56	Peak 2: 0.00	0.0	0.00
Conductivity (mS/cm): 0.0574	Peak 3: 0.00	0.0	0.00

Result quality **Good**

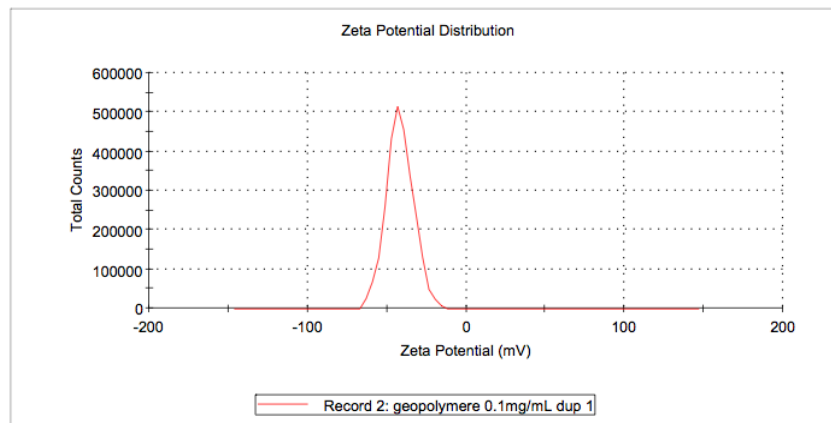


Figure 13 : Zeta potential of fly ash geopolymer in water

A negative value of zeta potential was identified assisting gel formation during geopolymerisation reaction. Indeed, when fly ash react with sodium hydroxide aqueous solution, the aluminate species form $[Al(OH)_4]^-$ and the silicate species form either $[SiO(OH)_3]^-$ or $[SiO_2(OH)_2]^{2-}$ [43], hence a negatively charged surface is formed while establishing a double layer. The Na^+ ions of the alkaline activator, will then react with these negatively charged surface groups and form a sodium aluminosilicate gel layer, $[Na_x(AlO_2)_x(SiO_2)_y.nNaOH.mH_2O]$, on their surfaces. The accumulation of more Na^+ ions in the double layer while forming gel resulted in a decrease of zeta potential. The value of Zeta potential found in this study agrees with the values of zeta potentials for some fly ash geopolymers synthesized by Gunasekara et al [44]. The authors have studied the factors affecting the performance of geopolymers made from a total of five chemically and physically distinct fly ashes. The values of zeta potential values for geopolymers are all negative and between -13,5 and -55 mV.

3.2.3 Water absorption

Water absorption is a vital property that stimuli the longevity of a building material. The lower water absorbed into geopolymeric material, the higher the resistance to water penetration and the lower the environmental damage caused on the material. Pitroda et al [45] stated that the movement of water through concrete structure is the main factor that will affect the durability of mortar and concrete. Due to this problem, the water absorption test is done to measure the absorb water in the concrete.

The water absorption is therefore a simple parameter to determine paste, mortar and concrete resistance to exposure in aggressive environments. In this study, the water absorption tests were carried out by immersing the

samples of geopolymer and ordinary portland cement pastes in water for 4 days and the percentage water absorbed was measured. The samples were immersed in water after 7, 14, 28 and 90 days of their elaboration. Table 5 gives the results of water absorption tests for fly ash geopolymer and Ordinary Portland cement paste (OPC) as control samples.

Table 5 . Water absorption of fly ash geopolymer and Ordinary Portland cement OPC pastes

Days	7	14	28	90
Water absorption% , geopolymer paste	16	12.4	9.3	7.2
Water Absorption% ; OPC paste	24	20	12	10

It was observed that after day 90, the samples have the lowest water absorption (7% for geopolymer sample and 10% for OPC sample). The samples have the highest water absorption at day 7 (16 % for geopolymer and 24% for OPC). The decrease of water absorption with time could be explained by the pore size decreases with time so, the structure of samples of geopolymer and OPC became denser and harder with time. The water absorption of fly ash geopolymer is smaller than that of OPC samples. The same result was obtained by Lurar et al [46]. The authors have studied the water absorption of concrete and found that the rate of water absorption is lesser in geopolymer concrete than in the control concrete. The water absorption is also related to compressive strength, Indeed, Thokchom et al [47] have conducted the study on the effect of water absorption on durability of fly ash based geopolymer mortars and found that the samples with higher water absorption have lowest compressive strength. It can be therefore concluded that pastes based on geopolymeric materials possess high resistance to aggressive environment and better compressive strength and durability than Ordinary portland cement.

The detailed study of the durability of fly ash geopolymer materials will be the subject of our futur work. The durability of fly ash based will be assessed through parameters related to the permeability, fire resistance, acid attack resistance and chloride and sulphate attack resistance.

Conclusion

The products resulting from the alkaline activation of Jorf Lasfar fly ashes exhibit an amorphous character with minority crystalline phases. The FTIR spectra reveal the differences between the raw fly ash and geopolymer binder when the main band corresponding to Si-O and Al-O vibrations is displaced towards lower values. In the ²⁹Si MAS NMR spectrum, these products exhibit a three-dimensional glassy structure with prevailing Q₄ (2-3Al) arrangement. The Al atoms penetrate into the original silicate structure of the fly ash during its alkaline activation and a new phase is formed.

The geopolymeric material is characterised by the heterogeneous matrix of geopolymeric gel and unreacted fly ash particles. Closed spherical pores are present, formed either as a result of the dissolution of original fly ash particles or by the air entrained during the preparation.

The fly ash geopolymers exhibit better performance than ordinary portland cements on water penetration and they possess very good fire resistance and can resist the effect of temperatures of up to about 800°C. The large value of potential zeta obtained indicates the high chemical stability of geopolymeric suspensions.

The properties of fly ash based geopolymer can be exploited for their application in the manufacture of cement , concrete, refractories, bricks ,ceramics, thermal insulating materials , sleepers of railways ,structures restoration and in several fields of civil engineering.

References

1. Davidovits J. , GEOPOLYMER Chemistry and Applications, 4th Edition, Institut Geopolymere (2015).
2. Verdolotti L., Iannace S., Lavorgna M., Lamanna R., *Journal of Materials Science*. 43(3)(2008) 865.
3. Lyon R. E., Balaguru P. N., Foden A., Sorathia U., Davidovics J., Davidovits M., *Fire and Materials*. 1 (1997) 67.
4. Giancaspro J., Balaguru P. N., Lyon R. E., Lopez-Anido R., *Journal of Materials in Civil Engineering* . 18 (3)(2006) 390.
5. Richard W.D.A., Riessen A.V.,Vickers LES. Fire-resistant geopolymers, Springer (2015).
6. Valeria F. F. B., Kenneth J. D. M., *Materials Letters*. 57 (2003) 1477.
7. Bell J., Gordon M., Kriven W. M., *Ceramic Engineering and Science Proceedings*. 26 (3) (2005) 407.
8. Zhang S. Z., Gong K. C., Lu H. W., *Materials Letters*. 58 (2004) 1292.

9. Li Z., Zhang Y., Zhou X., *Journal of Materials in Civil Engineering*. 17 (6) (2005) 624.
10. Hu M., Zhu X., Long F. J., *Cem. Concrete Compos.* 31 (2009) 762.
11. Fernandez-Jimenez A., Palomo A., *Fuel*. 82 (2003) 2259.
12. Fernandez-Jimenez A., de la Torre AG., Palomo A., Lopez-Olmo G., Alonso MM., Aranda MAG., *Fuel*. 85 (2006) 1960.
13. Fernandez-Jimenez A., Palomo A., *Cem. Concrete Res.* 35 (2005) 1984.
14. Criado M., Palomo A., Fernandez-Jimenez A., *Fuel*. 84 (2005) 2048.
15. Cheng T.W., Chiu J.P., *Minerals Engineering*. 16 (3) (2003) 205.
16. He J., Jie Y.X., Zhang J.H., Yu Y.Z., Zhang G.P., *Construction and Building Materials*. 30 (2012) 80.
17. Abdullah M.M.A., Hussin K., Bnhussain M., Ismail K.N., Ibrahim W.M.W., *Int. J. Pure Appl. Sci. Technol.* 6(1) (2011) 35-44.
18. Xu H., Van Deventer J. S. J., *International Journal of Mineral Processing*. 59(3) (2000) 247.
19. Skavara F., Jilek T., Kopecky L., *Ceramics-Silicaty*. 49 (3) (2005) 195.
20. Skavara F., Kopecky L., Nemecek J., Bittna Z. B., *Ceramics-Silicaty*. 50 (2006) 208.
21. Al Bakri A.M.M., Kamarudin H., Bnhussain M., Khairul N. I., Rafiza A.R., Zarina Y., *Journal of Engineering and Technology Research*. 3 (2) (2011) 44.
22. Palomo A., Grutzeck M.W., Blanco M.T. *Cem. Concrete Res.* 29 (8) (1999) 1323.
23. Andini S., Cioffi R., Colangelo F., Grieco T., Montagnaro F., Santoro L., *Waste Manage.* 28(2) (2008) 416.
24. Provis J.L., Duxon P., van Deventer J.S.J., *Adv. Powder Technol.* 21(1) (2010) 2.
25. Alonso S., Palomo A., *Cem. Concrete Res.* 31 (2001) 25.
26. Granizo M. L., Alonso S., Blanco-Varela M. T., Palomo A., *Journal of the American Ceramic Society*. 85 (1) (2002) 225.
27. Li X., Ma X., Zhang S., Zheng E. *Materials*. 6 (4) (2013) 1485.
28. Davidovits J. *Journal of Thermal Analysis*. 37 (8) (1991)1633.
29. Onisei S., Pontikes Y., Van Gerven T., Angelopolous G.N., Levea T., Predica V., Moldovan P. *J. Hazard. Mater.* (205-206) (2012) 101.
30. Nath D.C.D, Bandyopadhyay S., Gupta S., Yua A., Blackburn D., White C. *Applied Surface Science*. 256 (9) (2010) 2759.
31. Nayak P., Singh B. K., *Bull.Mater.Sci.* 30 (2007) 235.
32. Zhang Z., Wang H., Provis J.L., *Journal of Sustainable Cement-Based Materials*. 1(4) (2012) 154.
33. Khale D., Chaudhary R., *J. Mater. Sci.* 42 (2007) 729.
34. Alvarez-Ayuso E., Querol X., Plana F., Alastuey A., Moreno N., Izquierdo M., Font O., Moreno T., Diez S., Vazquez E., Barra M., *J. Hazard. Mater.* 154 (2008) 175.
35. Motorwala A., Shah V., Kammula R., Nannapaneni P., Raijiwala D.B., *IJETAE*. 3 (2013) 159.
36. Kramar S., Ducman V., *Chem. Ind. Chem. Eng. Q.* 21 (2014) 42.
37. Klinowski J. *Progress in NMR Spectroscopy*. 16 (1984) 237.
38. Bansal N. P., Singh J. P., Kriven W. M., Schneider H. *Ceram.Trans.* 153 (2003) 175.
39. Singh P.S., Bastow T., Trigg M. *Journal of Materials Science* 40 (2005) 3951.
40. Hoa J.P., McCormick P.G., Byrne L.T. *Journal of Material Science*. 37 (2002) 2311.
41. Kong D.L.Y., Sanjayan J.G., Sagoe-Crentsil K. *Cem. Concr. Res.* 37 (2007) 1583.
42. Cheng T.W., Chiu J.P. *Minerals Engineering*. 16 (3) (2003) 205.
43. Sagoe-Crentsil K., Weng L., *J. Mater. Sci.* 42(9) (2007) 3007.
44. Gunasekara C., Law D.W., Setunge S., Sanjayan J.G., *Construction and building materials*. 95 (2015) 592.
45. Pitroda J., Umrigar F.S., *International Journal of Engineering and Innovative Technology (IJEIT)*. 2(7) (2013) 245.
46. Luhar S., Khandelwal U., *International Journal of Civil Engineering (SSRG-IJCE)* 2 (8) (2015) 1-10.
47. Thokchom S., Ghosh P., Ghosh S., *ARPN Journal of Engineering and Applied Sciences*. 4 (2009) 28.

(2017) ; <http://www.jmaterenvironsci.com>